Journal of the European Ceramic Society 17 (1997) 1239–1246

PII:S0955-2219(96)00219-1
0955-2219/96/$15.00

Preparation of an Aluminium Titanate–25 vol% Mullite Composite by Sintering of Gel-Coated Powders

Y. X. Huang, A. M. R Senos and J. L. Baptista

Departamento de Engenharia Cerâmica e do Vidro, INESC/Universidade de Aveiro, 3810 Aveiro, Portugal

(Received 10 June 1996; accepted 21 October 1996)

Abstract

A gel-coated powder processing, i.e. mullite precursor gel coating synthesised Al_2TiO_5 solid solution (with 2·5 wt% MgO) particles, was used to prepare an Al_2TiO_5–25 vol% mullite composite precursor. The mullitisation, densification, mechanical and thermal properties of the composite have been investigated. It was found that direct mullitisation occurred at 988°C in the composite precursor this being attributed to the presence of Al_2TiO_5 particles. Two different mullite morphologies with near isometric and acicular shapes were observed. The formation of acicular mullite is ascribed to the presence of a liquid phase at the firing temperature as a consequence of composition alterations due to segregation of Al_2O_3 and SiO_2. Good dispersion of the mullite grains along the grain boundaries was observed in samples that attained high densification. The thermal expansion coefficient of the composite was still relatively low (~2·7 × $10^{-6}K^{-1}$). During long-term (100 h at 1100°C) decomposition tests the Al_2TiO_5 chemical stability was maintained. © *1996 Elsevier Science Limited.*

1 Introduction

A low thermal expansion coefficient (TEC) and a high thermal shock resistance are important for materials when they are used in severe thermal environments. Aluminium titanate (Al_2TiO_5) has been recognised as a low TEC material for several decades.[1–3] However, industrial application of this material has been hindered by two well-recognised problems: first, the very weak mechanical strength due to thermal anisotropy-induced microcracking,[4] and second the decomposition of Al_2TiO_5 into α-Al_2O_3 and TiO_2 (rutile) between about 800°C and 1280°C.[5] Some oxide dopants like MgO, SiO_2, Fe_2O_3, SnO_2, CaO, and other rare-earth oxides have been used to control the decomposition of Al_2TiO_5.[6] Only MgO and Fe_2O_3 seem to produce phase stability by the formation of intermediate phases such as magnesium titanate or iron titanate first and then a solid solution between Al_2TiO_5 and the as-formed intermediate phases.[7] However long-term stability is still hard to achieve.

The importance of the recently developed Al_2TiO_5–mullite composites[8–10] (or other systems such as ZrO_2–Al_2TiO_5 and $ZrTiO_4$–Al_2TiO_5[11,12]) is that such composites offer a compromise between the low strength and low thermal expansion of Al_2TiO_5 and the good strength and moderate expansion of mullite providing thus an opportunity to tailor the required properties through the selection of composite compositions. For instance, strengths as high as ~230 MPa were reported[13] in the Al_2TiO_5–mullite system when it contained ~30 wt% Al_2TiO_5. This is a big improvement in the mechanical strength compared with those quoted for single-phase Al_2TiO_5 (typically, 5–10 MPa), although the favourable TEC value of Al_2TiO_5 ($\leq 1 \times 10^{-6}K^{-1}$) was also increased to ~7 × $10^{-6}K^{-1}$, between 20 and 1000°C. When the amount of Al_2TiO_5 was increased, the mechanical strengths for the corresponding composites decreased, but were still around 80 MPa at 75 wt% Al_2TiO_5 with a TEC of ~3·5 × $10^{-6}K^{-1}$. However, lower strength values were quoted by Freudenberg *et al.*[14] who studied the thermal stability of the same system as in Ref. 13 and obtained strengths of ~50 MPa. This variation in mechanical strength values present in the literature serves to illustrate that the engineering properties of Al_2TiO_5-based composites depend not only on the composite composition, but on the processing variables and consequent microstructure control as well.

The preparation of Al_2TiO_5-based composite powders by different methods, namely conventional methods using oxide mixtures[12] and sol–gel

methods,[9,10] has been attempted. Most of them use reaction sintering where difficulties such as densification are generally encountered, especially when a high Al_2TiO_5 content is involved. Few groups[13] have tried to use synthesised Al_2TiO_5 powder to prepare Al_2TiO_5–mullite powders, but the understanding of the process remained insufficient, especially for mullitisation processes and its correlation to microstructure.

In the present work, a synthesised Al_2TiO_5 powder (containing 2·5 wt% MgO, on the weight of Al_2TiO_5), aluminium *sec*-butoxide and tetraethylorthosilicate were used to prepare Al_2TiO_5–25 vol% mullite composite powders by the gel-coated method, i.e. Al_2O_3 and SiO_2 gels coating Al_2TiO_5 particles. Similar powder processing has been attempted in other composite systems[15,16] to control microstructure. The selection of this composition is based on the expection that near this composition point an improved mechanical strength will be achieved without great deterioration of the Al_2TiO_5 favourable low TEC and high thermal shock resistance.

2 Experimental Procedure

The synthesis of the Al_2TiO_5 powder was carried out by first mixing the α-Al_2O_3 powder (0·2 μm mean particle size, Alcoa Reagents), TiO_2 powder (0·8 μm mean particle size, Merck Reagents) and $Mg(NO_3)_2{\cdot}6H_2O$ in a planetary ball mill for 2 h, using absolute ethanol as the milling medium. The slurry obtained was dried in an oven at 80°C during 12 h, heated at 1300°C for 1 h, and finally ball milled for 6 h, using again absolute ethanol as the milling medium. The X-ray diffraction patterns for the powder obtained have shown that Al_2TiO_5 solid solution is the dominant phase. Aluminium *sec*-butoxide ($Al(OC_4H_9)_3$, Merck Reagents) and tetraethylorthosilicate ($Si(OC_2H_5)_4$, TEOS, Fluka Chimie AG) were used as sources of mullite. After weighing, they were dissolved in absolute ethanol. The synthesised Al_2TiO_5 powder was added into the solution based on the volume ratio Al_2TiO_5: mullite = 75:25. The hydrolysis of $Al(OC_4H_9)$ and TEOS was carried out by adding five times the equivalent water to the suspension. Strong mechanical stirring was used during the whole processing. After stirring for 1 h, the mixture was dried in an oven at a temperature of 80°C.

The as-obtained precursor was characterised by a differential scanning calorimetry (DSC, Netzsch STA 404C model) at a heating rate of 10°C/min up to 1400°C with α-Al_2O_3 as the reference material. The thermogravimetric analysis (TGA) curve was also recorded by the same instrument. After, the composite precursor was calcined at 500°C for 1 h, the resulting powder was pressed into bars (3·5 × 5 × 50 mm^3) by first uniaxial pressing at 50 MPa and then isostatic pressing under 200 MPa pressure. Sintering was performed in a box furnace, at a heating rate of 5°C min^{-1} up to a setting temperature, holding 4 h and then the samples were cooled down at a constant rate of 5°C/min until ~500°C.

The X-ray diffraction analysis (XRD) was carried out in a diffractometer (D/max-C, Rigaku) using Cu K_α radiation, voltage 40 kV, electric current 20 mA. The powders for the XRD experiments were obtained by heating the precursor to various temperatures, holding 1 h and then cooling down quickly, or by grinding the sintered bodies into powder. The morphology of the composite powder and sintered specimens was observed by scanning electron microscopy (SEM, Hitachi, S-4100) using the secondary electron or the backscatter modes. Energy dispersive microanalysis (EDX) was done for the same samples. The average grain size, expressed as a mean diameter of area, was measured by an image processing program.

The shrinkage behaviour of the powder compact was recorded with a dilatometer (Linseis series), at a heating rate of 5°C min^{-1} up to 1450°C with a soaking time of 4 h. The density was determined by mercury displacement. The corresponding densification curve was calculated using the measured green density as the initial reference and assuming isotropic shrinkage. The thermal expansion behaviour of the sintered body was measured with the same instrument at a constant heating rate of 5°C min^{-1} up to 1400°C and then cooling down to 500°C at a speed of 5°C min^{-1}. The thermal stability test for the composite was carried out by annealing the sample at 1100°C in air for 100 h followed by identifying the crystalline phases present.

A Shimadzu testing machine (Autograpa, AG-A series) was used to measure the three-point flexural strength. The specimens were polished with silicon carbide abrasive paper (No. 1000) before measurements. The typical sample dimension is 2·5 × 3·5 × 40 mm^3. The span length was 20 mm and the crosshead speed 0·5 mm min^{-1}. Young's modulus was calculated from the linear parts of the stress-strain curves. Each data point is the average of 4–5 bars.

3 Results and Discussion

3.1 Mullite phase formation

Figure 1 gives the DSC-TGA curves for the composite precursor. The endothermic peak at ~60°C,

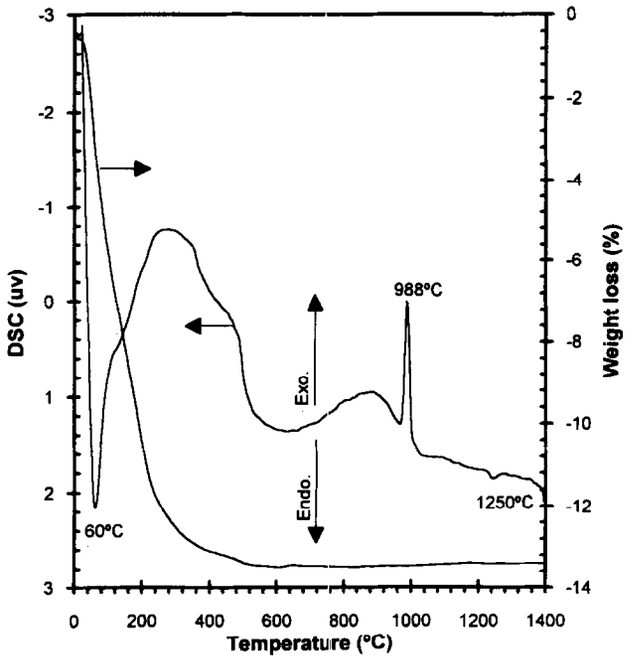

Fig. 1. DSC-TGA curves for the composite precursor, at a heating rate of 10°C min^{-1}.

which is associated with a big weight loss, is attributed to the removal of the absorbed water and remaining ethanol. The following broad exothermic peak between about 100 and 600°C is a consequence of the oxidation of organic residues. In this temperature range, there is an ~8% weight loss. No further weight loss is observed above 600°C; however, the DSC curve shows a strong, sharp exothermic peak at 988°C, which is attributed to the crystallisation of the so-called pseudotetragonal mullite. The difference between the poorly crystallised pseudotetragonal and well-crystallised orthorhombic mullite, which can be distinguished by taking X-ray diffractograms, is that the (120) and (210) peaks of orthorhombic mullite are distinctly split, and that no splitting is observed for the pseudotetragonal mullite.[17] The XRD patterns for the powders heated at 900°C, 1050°C and 1300°C are shown in Fig. 2. Mullite has already been formed in the sample heated at 1050°C. The main peak of mullite is overlapped by the main, strong (101) peak of β-Al_2TiO_5. No splitting of the orthorhombic (120) and (210) peaks is observed, which is indicative of the formation of pseudotetragonal mullite at this temperature. When the temperature is increased up to 1300°C, the (120) peak of orthorhombic mullite separates from the main peak of β–Al_2TiO_5 (the (210) peak of orthorhombic mullite is still overlapped by the (101) line of Al_2TiO_5), indicating that pseudotetragonal mullite has been transformed into orthorhombic mullite. In the DSC curve of Fig. 1, there is a small endothermic peak at 1250°C, which indicates the formation of Al_2TiO_5 from the remaining α-Al_2O_3 and TiO_2

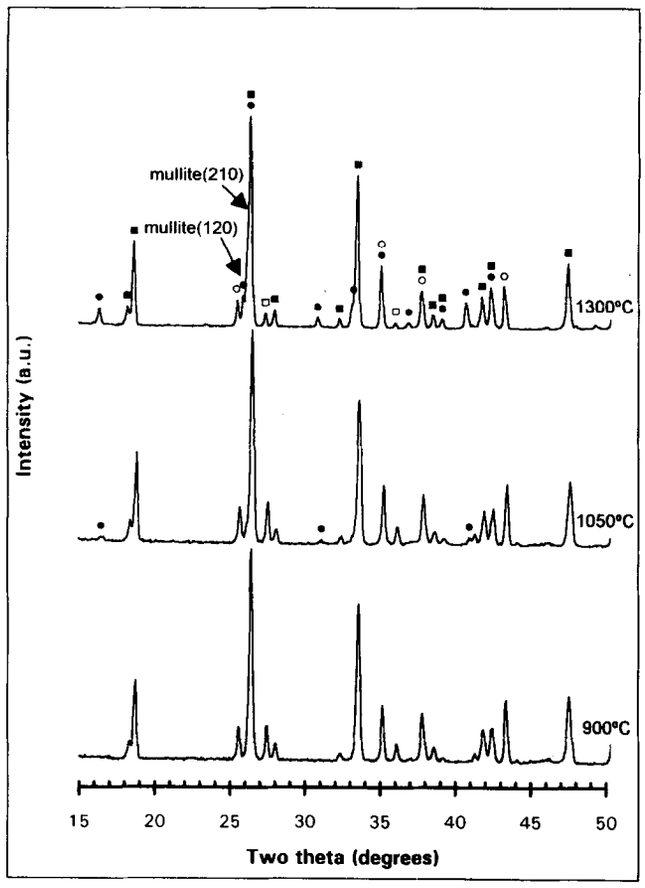

Fig. 2. XRD patterns of the composite powders heated at 900, 1050 and 1300°C for 1 h. (●) mullite, (■) β-Al_2TiO_5; (○) α-Al_2O_3; (□) rutile).

(rutile) in the starting Al_2TiO_5 powder. This is confirmed by the observation of a reduced XRD peak intensity for both α-Al_2O_3 and TiO_2 (rutile) in the sample calcined at 1300°C.

The explanation for mullite formation is still open to controversy,[18–20] especially for the exothermic reaction at ~1000°C. γ-Al_2O_3 spinel (or Al-Si spinel) and mullite or a mixture of them are believed to be associated with that exotherm, although it is known that its presence depends on variations of the initial raw materials or the techniques of preparation. It is important to note that the ~1000°C exotherm associated with the formation of mullite is generally observed in monophasic mullite precursors, where a mixing scale of Al_2O_3 and SiO_2 components in a molecular level was assumed. In the present case it might be that the presence of Al_2TiO_5 can favour the nucleation of mullite because of their similar crystal structures. Huling and Messing[21] found that the seeding of crystalline mullite particles indeed can lower the mullitisation temperature, although the effectiveness was limited in their case.

3.2 Power morphology

Microphotographs of the Al_2TiO_5 powder, the composite precursor and calcined composite

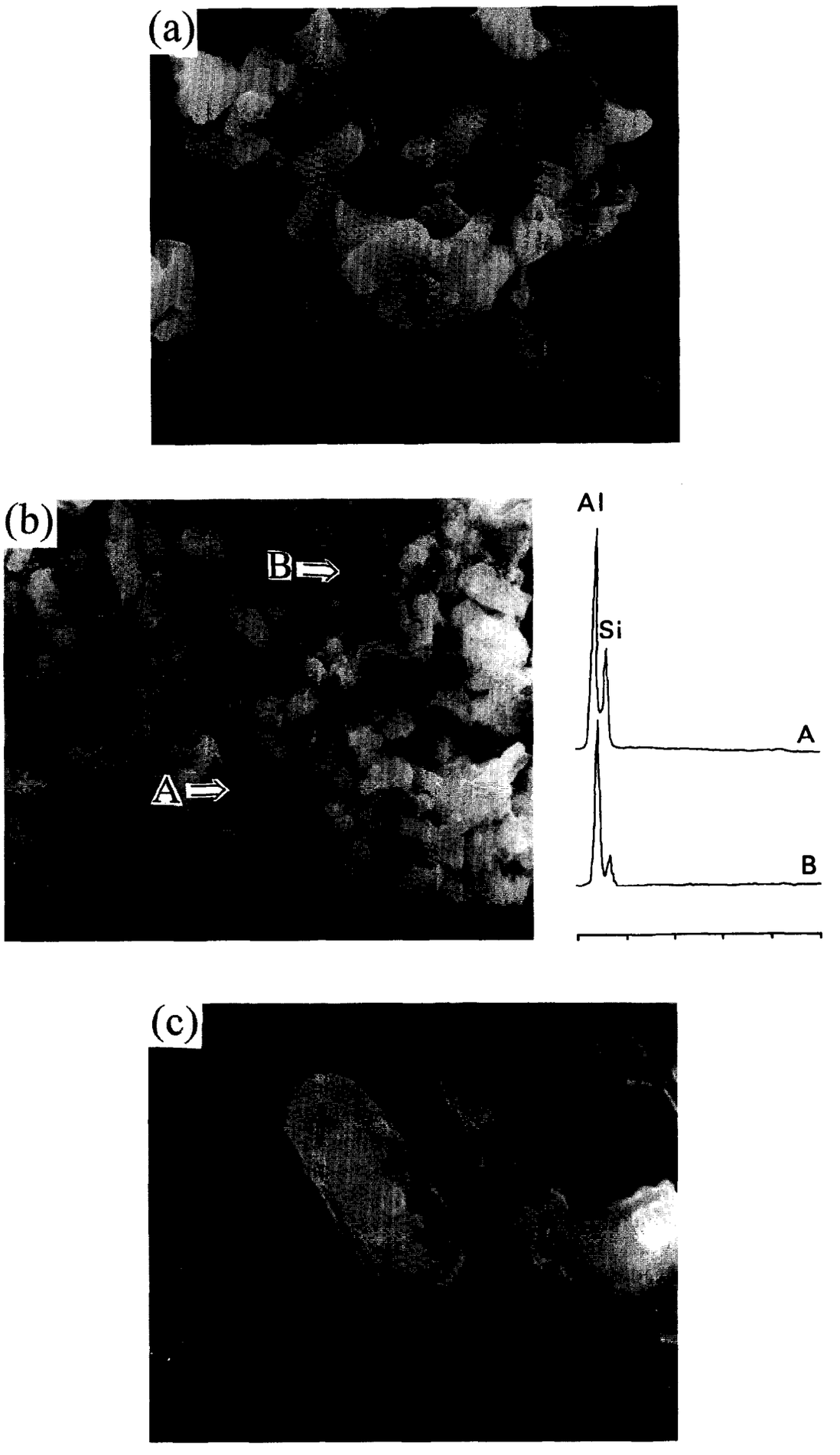

Fig. 3. SEM photographs of the powders and EDX spectra of the designated points. (a) The starting Al_2TiO_5 powder; (b) the composite precursor; (c) the calcined composite powder.

powder are depicted in Fig. 3. The starting Al_2TiO_5 (Fig. 3(a)) particles have approximately prismatic shapes. The average particle size is about 3 μm. When the Al_2TiO_5 powder was dispersed in the ethanolic solution of $Al(OC_4H_9)_3$ and $Si(OC_2H_5)_4$ and the subsequent hydrolysis was accomplished, the resulting Al_2O_3 and SiO_2 gels coated the surfaces of many Al_2TiO_5 particles, as observed in the microphotograph of the composite precursor (Fig. 3(b)). This is confirmed by the corresponding point EDX analysis, which also shows the heterogeneity of Al_2O_3 and SiO_2 components in the mullite precursor. Apparently, the well-dispersed Al_2TiO_5 particles in the mullite precursor can effectively prevent Al_2O_3 and SiO_2 gel particles from forming big agglomerates. Figure 3(c) for the calcined powder shows that the dehydrated Al_2O_3 and SiO_2 particles still stay on the surfaces of Al_2TiO_5 particles after heat treatment. This powder structure is important to yield the required microstructure during subsequent firing.

3.3 Sintering and microstructure

The sintering of the powder compact was carried out at temperatures of 1350°C, 1450°C and 1550°C during 4 h. The results are shown in Table 1. A quite dense sample with an ~97% of theoretical density was achieved when it was fired at 1450°C for 4 h. The sample sintered at 1550°C has a lower relative density. The theoretical density was estimated from the initial composition (assuming that the reactions of mullite and Al_2TiO_5 are complete) with the values of 3·17 g cm^{-3} and 3·70 g/cm^{-3} respectively for the theoretical density of mullite and Al_2TiO_5. The detailed densification behaviour was also monitored by dilatometry, as shown in Fig. 4. Densification begins at about 950°C, followed by two plateaux starting at about 980°C and 1235°C, respectively. The former is attributed to the mullitisation process. Densification slows down although no obvious volume change is associated with this process, confirming that phase transformation can influence densification kinetics.[22–24] The latter is due to the formation of a little amount of Al_2TiO_5 from the remainder of rutile and α-Al_2O_3 in the starting Al_2TiO_5 powder. Both are consistent with the observation of the ~988°C exothermic peak and ~1250°C endothermic peak in the previous DSC curve. After that, densification proceeds at a faster

Table 1. Relative density of the composite sample sintered at various temperatures with a soaking time of 4 h

Sintering temperature (°C)	*1350°C*	*1450°C*	*1550°C*
Relative density (%)	86·4	96·7	91·1

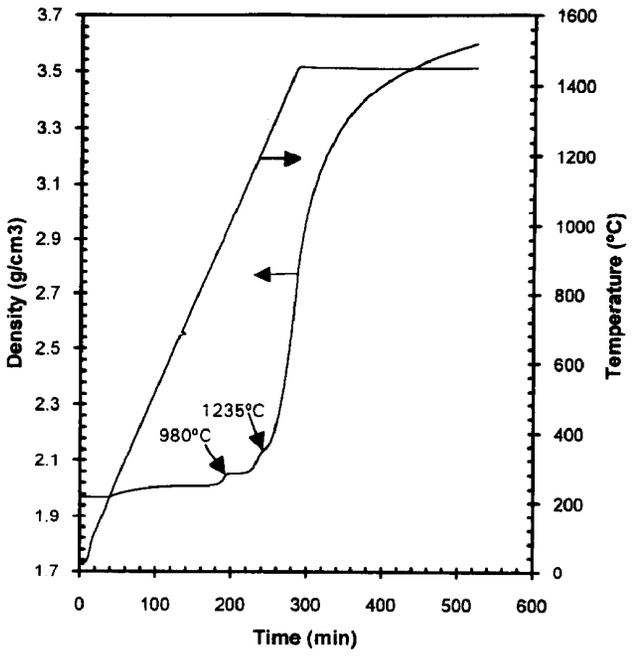

Fig. 4. Densification curve of the composite sample, at a heating rate of 5°C min^{-1} up to 1450°C, with a soaking time of 4 h.

rate as a consequence of the sintering of both Al_2TiO_5 and mullite. A dense composite was achieved after 4 h at 1450°C. Unlike other composite systems in which densifications are generally retarded by introduction of second phases,[25,26] the enhanced densification in the present system is probably due to: (1) the use of pre-synthesised Al_2TiO_5 powder which can avoid the occurrence of large size Al_2TiO_5 'domains', which were widely observed in reaction-sintered Al_2TiO_5 due to the rapid grain growth of Al_2TiO_5;[6,25] (2) the formation of a grain boundary liquid phase due to the presence of SiO_2.[6,27]

Microphotographs of two representative areas of the composite specimen sintered at 1450°C for 4 h are shown in Figs 5(a) and (b). The photographs were taken in the backscatter mode, where the Al_2TiO_5 grain is white and mullite is grey. The Al_2TiO_5 mean grain size is about 3·5 μm. This is very close to that in the starting powder because the synthesised Al_2TiO_5 particles will be quite inert during sintering since the mullite second phase would restrain the grain growth during the sintering of the composite. Two different morphologies for mullite grains are observed. One is the near isometric mullite grains about 2 μm in size and the other is prismatic mullite grains about 0·5 to 1·5 μm wide becoming acicular in shape. They are mainly located at grain boundaries or triple points of the Al_2TiO_5 matrix. Formation of these two features of mullite morphology depends on the mullite composition in the gel. Pask *et al.*[27] also observed these two different shapes of mullite grains in their stoichiometric mullite precursors

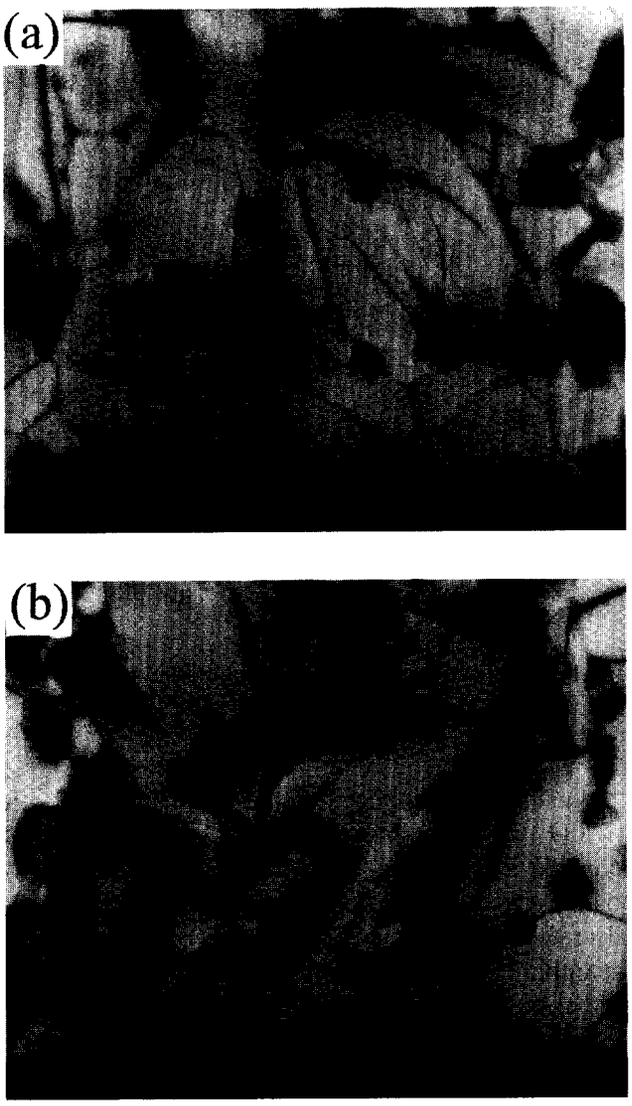

Fig. 5. SEM photographs of the representative areas in the composite sample sintered at 1450°C for 4 h in the back-scattered mode, sharing two different mullite morphologies.

and postulated that the formation of acicular mullite is due to the presence of a liquid phase at the firing temperature and that the near isometric shape mullite forms in the absence of liquid phase. In the present case, the formation of these two different shapes of mullite could be associated with Al_2O_3 and SiO_2 composition differences in the mullite precursors. The point EDX analysis in Fig. 3 verified that some parts of the precursor are SiO_2-rich. Probably, the acicular mullite was formed in SiO_2-rich regions due to the presence of a liquid phase at the firing temperature, whereas near isometric mullite formed in other regions. The acicular mullite morphology is particularly beneficial to hinder crack propagation.

3.4 Physical properties

The physical properties of the aluminium titanate–25 vol% mullite composites prepared in this work are given in Table 2. An improved flexural strength was obtained for the composite sample compared with the typical strength values for pure Al_2TiO_5.[6] This could be linked to the microstructure observed in Fig. 5: (i) a small Al_2TiO_5 grain size is obtained in the composite sample due to the use of synthesised and coated Al_2TiO_5 powder and the suppressed grain growth effect by the mullite phase; (ii) many fewer microcracks are initiated along grain boundaries and within grains in the composite sample; (iii) the formation of the acicular mullite grains on grain boundaries during sintering could effectively hinder the progress of an advancing crack. It is probable that a combination of all these mechanisms contributes to the increased mechanical strength.

The expansion behaviour in heating and cooling for the sintered composite sample is shown in Fig. 6. The curve exhibits a pronounced hysteresis loop, which has been considered to be the characteristic of anisotropic materials or composite materials having phases with different expansion coefficients in which large stresses are easily developed. As observed in Fig. 5, microcracks are present within grains or along grain boundaries. They probably formed during the cooling stages due to the severe thermal expansion coefficient anisotropy of the individual Al_2TiO_5 grain and the difference in TEC between Al_2TiO_5 and mullite. When the sample is heated again, the as-formed microcracks will be healed, and thus a low thermal expansion could be observed. The thermal expansion increases after the closure of microcracks. During the cooling stage, the sample shrinks quickly due to the high average thermal expansion coefficient. At a low temperature, microcracks will open up again, resulting in a reduced shrinkage process. The turning point temperature, which was not precisely identified within the experimental temperature range, is less than 500°C. Such a low temperature is due to the improved mechanical strength.

Table 2. Physical properties of the aluminium titanate mullite composite sintered at 1450°C for 4 h

Green density ($g\ cm^{-3}$)	*Al_2TiO_5 grain size (μm)*	*Mullite grain size (μm)*	*Sintering density (g/cm^{-3})*	*Flexural strength (MPa)*	*Young's modulus E (GPa)*	*Thermal expansion coefficient $\alpha_{20-1000°C}$ ($10^{-6}K^{-1}$)*	*Thermal shock resistance R_1 (K)*
1·97	3·7	2·6	3·48	80·7 ± 6·8	12·93	2·67	1566

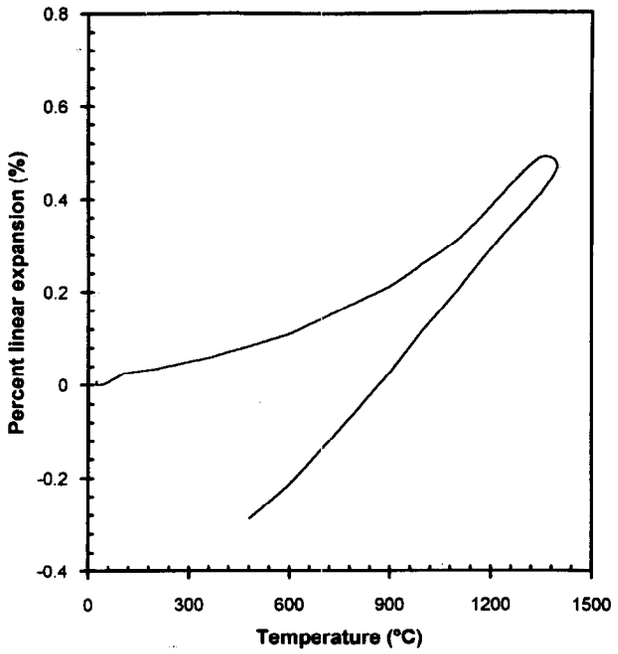

Fig. 6. Thermal expansion curve of the composite sintered sample, at a heating and cooling rate of 5°C min^{-1}, in air.

The thermal shock resistance parameter R_1 shown in Table 2 was evaluated by the following relation:[28]

$$R_1 = \Delta T = \sigma(1-\mu)/\alpha E$$

where R_1 is the thermal shock resistance parameter, σ the flexural strength, E the Young's modulus, α the thermal expansion coefficient, and μ the Poisson's ratio, which is assumed to be 0·33. From the equation above, the avoidance of fracture initiation is required to obtain a high thermal shock resistance. The high R_1 value of the composite sample is due to the low thermal expansion coefficient and the improved mechanical strength.

The thermal decomposition behaviour of the Al_2TiO_5 in the composite was checked by annealing the sintered composite sample at 1100°C in air for 100 h, where the decomposition rate of the Al_2TiO_5 solid solution is fastest,[29] and then grinding the sample into powder. The XRD results for the powders before and after the thermal treatment test are shown in Fig. 7. Only a trace of rutile was observed after the test, indicating that the thermal stability of Al_2TiO_5 was maintained. The presence of both SiO_2 and MgO is responsible for the thermal stability.

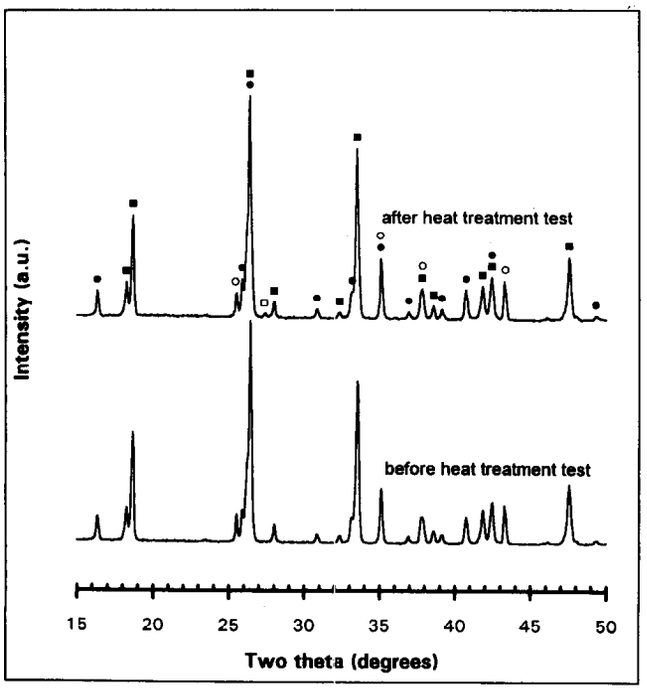

Fig. 7. XRD patterns for the composite sample sintered at 1450°C, for 4 h, and after heat treatment test at 1100°C for 100 h. (●) mullite; (■) β-Al_2TiO_5; (○) α-Al_2O_3; (□) rutile.

4 Conclusions

In the present investigation, a gel-coated powder processing method, i.e. a mullite precursor gel coating pre-synthesised Al_2TiO_5 solid solution particles, was used to prepare Al_2TiO_5–25 vol% mullite composite.

Mullite was directly formed by an exothermic reaction at ~980°C and two different morphologies of mullite grains were observed. A microstructure with a good dispersion of mullite grains in the Al_2TiO_5 matrix was achieved.

The composite shows an improved mechanical strength over pure Al_2TiO_5 ceramics. The improved strength is attributed to the enhanced densification and the good dispersion of mullite grains along Al_2TiO_5 grain boundaries.

The thermal expansion coefficient of the composite is maintained at a low value and long-term (100 h at 1100°C) chemical stability of the Al_2TiO_5 phase in this composite was achieved.

Acknowledgements

The authors gratefully acknowledge the financial support from JNICT through the research project PBIC/C/CTM/1947/95.

References

1. Lang, S. M., Fillmore, C. L. and Maxwell, L. H., The system beryllia–alumina–titania: phase relations and general physical properties of three-component porcelains. *Res. Natl Bur. Stand.*, 1952, **48**, 298–312.
2. Morosin, B. and Lynch, R. W., Structure studies on Al_2TiO_5 at room temperature and at 600°C. *Acta Cryst.*, 1972, **B28**, 1040–1046.
3. Hennicke, H. W. and Lingenberg, W., The formation and decomposition of aluminium titanate: II, the decomposition reaction of aluminium titanate. *cfi/Ber.DKG*, 1986, **63**, 100–106.

4. Thomas, H. A. J. and Stevens, R, Aluminium titanate—a literature review: part 1, microcracking phenomena. *Br. Ceram. Trans. J.*, 1989, **88**, 144–151.
5. Kato, E., Daimon, K. and Takahashi, J., Decomposition temperature of β-Al_2TiO_5. *J. Am. Ceram. Soc.*, 1980, **63**, 355–356.
6. Thomas, H. A. J. and Stevens, R., Aluminium titanate—a literature review: part 2, engineering properties and thermal stability, *Br. Ceram. Trans. J.*, 1989, **88**, 184–190.
7. Buscaglia, V., Nanni, P., Battilana, G., Aliprandi, G. and Carry, C., Reaction sintering of aluminium titanate: I—effect of MgO addition. *J. Eur. Ceram. Soc.*, 1994, **13**, 411–417.
8. Yano, T., Kiyohara, M and Otsuka N., Thermal and mechanical properties of aluminium titanate — mullite composites: part 3, effects of aluminium titanate particle size. *J. Ceram. Soc. Japan*, 1992, **100**, 482–487.
9. Morishima, H., Kato, Z., Uematsu, K., Saito, K., Yano, T. and Ootsuka, N., Synthesis of aluminium titanate—mullite composite having high thermal shock resistance. *J. Mater. Sci. Lett.*, 1987, **6**, 389–390.
10. Kim, J., Zografou, C. and Krönrt, W., Thermal shock resistant materials based on aluminium titanate–mullite composites. In *Proceedings of the Unified International Technical Conference on Refractories*, Aachen, 1991, 2nd edn, ed. German Refractories Association, Stahl und Eisen, 1992, 197–201.
11. Parker, F. J., Al_2TiO_5–$ZrTiO_4$–ZrO_2 composites: a new family of low-thermal expansion ceramics. *J. Am. Ceram. Soc.*, 1990, **73**, 929–932.
12. Wohlfromm, H., Moya, J. S. and Pena, P., Thermal shock behaviour of aluminium titanate based materials. In *Proceedings of the Third European Ceramic Society Conference*, ed. P. Duran and J. F. Fernandez. Faenza Editrice Iberica S. L., Spain, 1993, 1003–1012.
13. Yano, T., Nagai, N., Kiyohara, M., Saito, K. and Otsuka, N., Thermal and mechanical properties of aluminium titanate–mullite composites: part 1, effects of composition. *Yogyo - Kyokai - Shi*, 1986, **94**, 970–976.
14. Freudenberg, B. and Seyer, J., Sintered ceramic materials based on aluminium titanate: a process for their production and their use. US Patent 5153153, 6 Oct. 1992.
15. Wang, C. M. and Riley, F. L., Alumina coating silicon nitride powders. *J. Eur. Ceram. Soc.*, 1992, **10**, 83–93.
16. Kulig, M., Oroschin, W. and Greil, P., Sol–gel coating of silicon nitride with Mg–Al oxide sintering aid. *J. Eur. Ceram. Soc.*, 1989, **5**, 209–217.
17. Schneider, H. and Rymon-Lipinski, T., Occurrence of pseudotetragonal mullite. *J. Am. Ceram. Soc.*, 1988, **71**, c-162–c-164.
18. Schneider, H., Merwin, L. and Sebald, A., Mullite formation from non-crystalline precursors. *J. Mater. Sci.*, 1992, **27**, 805–812.
19. Schneider, H., Saruhan, B., Voll, D., Merwin, L. and Sebald, A., Mullite precursor phases. *J. Eur. Ceram. Soc.*, 1993, **11**, 87–97.
20. Chakravorty, A. K., Effects of pH on 980°C spinel phase-mullite formation of Al_2O_3–SiO_2 gels. *J. Mater. Sci.*, 1994, **29**, 1558–1568.
21. Huling, J. C. and Messing, G. L., Epitactic nucleation of spinel in aluminosilicate gels and its effect on mullite crystallisation. *J. Am. Ceram. Soc.*, 1991, **74**, 2374–2381.
22. Lequeux, N., Bonhomme-Coury, L., Mussotte, S. and Boch, P., Reaction sintering of ZrO_2–Al_2TiO_5 composites. In *Proceedings of the Third European Ceramic Society Conference*, ed. P. Duran and J. F. Fernandez. Faenza Editrice Iberica S. L., Spain, 1993, 1011–1016.
23. Thomas, H. A., Stevens, R. and Gilbart, E., Effect of zirconia additions on the reaction sintering of aluminium titanate. *J. Mater. Sci.*, 1991, **26**, 3613–3616.
24. Freudenberg, B. and Mocellin, A., Aluminium titanate formation by solid-state reaction of fine Al_2O_3 and TiO_2 powders. *J. Am. Ceram. Soc.*, 1987, **70**, 33–38.
25. Messing, G. L. and Onoda, G. Y., Sintering of inhomogeneous binary powder mixtures. *J. Am. Ceram. Soc.*, 1981, **64**, 468–472.
26. Bordia, R. K. and Raj, R., Sintering of TiO_2–Al_2O_3 composites: a model experimental investigation. *J. Am. Ceram. Soc.*, 1988, **71**, 302–310.
27. Pask, J. A., Zhang, X. W. and Tomsia, A. P., Effect of sol–gel mixing on mullite microstructure and phase equilibria in the α-Al_2O_3–SiO_2 system. *J. Am. Ceram. Soc.*, 1987, **70**, 704–707.
28. Kingery, W. D., Bowen, H.K and Uhlmann, D. R., *Introduction to Ceramics*. John Wiley & Sons, New York, 1975, 609.
29. Ishitsuka, M., Sato, T., Endo, T. and Shimada, M., Synthesis and thermal stability of aluminium titanate solid solutions. *J. Am. Ceram. Soc.*, 1987, **70**, 69–71.